Uncertainty and Disturbance Estimator-Based Backstepping Control for Nonlinear Systems With Mismatched Uncertainties and Disturbances

Jiguo Dai
Department of Mechanical Engineering,
Texas Tech University,
Lubbock, TX 79409
e-mail: jiguo.dai@ttu.edu

Beibei Ren[1]
Department of Mechanical Engineering,
Texas Tech University,
Lubbock, TX 79409
e-mail: beibei.ren@ttu.edu

Qing-Chang Zhong
Department of Electrical & Computer Engineering,
Illinois Institute of Technology,
Chicago, IL 60616
e-mail: zhongqc@ieee.org

This paper proposes an uncertainty and disturbance estimator (UDE)-based controller for nonlinear systems with mismatched uncertainties and disturbances, integrating the UDE-based control and the conventional backstepping scheme. The adoption of the backstepping scheme helps to relax the structural constraint of the UDE-based control. Moreover, the reference model design in the UDE-based control offers a solution to address the "complexity explosion" problem of the backstepping approach. Furthermore, the strict-feedback form condition in the conventional backstepping approach is also relaxed by using the UDE-based control to estimate and compensate "disturbance-like" terms including nonstrict-feedback terms and intermediate system errors. The uniformly ultimate boundedness of the closed-loop system is analyzed. Both numerical and experimental studies are provided. [DOI: 10.1115/1.4040590]

Keywords: uncertainty and disturbance estimator, backstepping, mismatched uncertainties and disturbances

1 Introduction

The control problem for uncertain systems has been widely studied by a variety of strategies. Among them, the time delay control (TDC) is proposed in Ref. [1], which is based on the assumption that a continuous signal remains unchanged during a small enough period. By using the past observation of uncertainties and disturbances, the control action is modified directly, instead of adjusting controller gains (e.g., gain scheduling), or identifying system parameters (e.g., adaptive control). Although the TDC has been successfully applied to different applications [2–6], it suffers from some problems, which are caused by the need for the derivatives of system states and the difficulty in stability analysis due to the use of time-delayed signals.

To address the above problems in the TDC, an alternative strategy, which is named by uncertainty and disturbance estimator (UDE)-based control, is proposed in Ref.[7]. Inheriting from the TDC control, the UDE-based control has the similar structure but uses the assumption in the frequency domain that a continuous signal can be approximated by appropriately filtering. Since then, both theoretical and practical studies on the UDE-based control begin to appear in the literature. In the aspect of theoretical studies, the two-degrees-of-freedom nature of the UDE-based control is revealed in Ref. [8], which indicates that the UDE-based control strategy can be decoupled into two designs, i.e., one is a reference model with an error feedback matrix and the other one is a filter. The reference model with the error feedback gain matrix determines the system output performance, and the filter design determines the performance of uncertainties and disturbances rejection. Due to the importance of the filter design, Shendge and Patre, Chandar and Talole, Kuperman, and Ren et al. [9–12] have discussed how to improve the filter design in the UDE-based control to achieve a better disturbance rejection performance. In Ref. [13], a robust input–output linearization controller is reported by using the UDE-based control technique. Furthermore, an UDE-based controller–observer structure is proposed by constructing a Luenberger type state observer in Ref. [14]. A new design of sliding mode control based on the UDE is given in Ref. [15], and the UDE-based control successfully avoids the control discontinuity and the need for the bounds of the uncertainties, which are main difficulties in the conventional sliding mode control. The robust design for an UDE-based controller with a reduced order observer is studied in Ref. [16]. In addition, to overcome the large initial control signal in the UDE-based control, a novel change of coordinates is also presented in Refs. [15] and [17]. Moreover, by regarding varieties of nonlinearities as the uncertainties and disturbances, the UDE-based control has been extended to systems with state delays [18,19], nonaffine input [20], coupling states [21], hysteresis effect [22], etc.

Benefiting from the excellent performance in handling the uncertainties and disturbances is yet a simple control scheme, the UDE-based control has been applied to many types of practical systems in recent years, such as robot manipulators [23], aeroengine [24], wind turbine systems [25], wing rock motion [26], DC-DC converters [27], quadrotors [21], grid-connected inverters [28], VTOL aircraft [29], power plant [30]. However, it should be noted that the structural constraint [7], that is equivalent to the matching condition of *uncertainties and disturbance*s, has not been relaxed yet in the UDE-based control, which restricts the further application of the UDE-based control to some systems with mismatched uncertainties and disturbances. To fill in the gap and broaden the applicability, this paper aims to relax the structural constraint of the UDE-based control by using the backstepping scheme.

In the view of the backstepping approach, the controller is derived in a recursive process, that is, the lower order subsystem state is stabilized by a virtual control which will be designed in the higher order subsystem. Henceforth, the backstepping approach is promising to handle the mismatched uncertainties [31]. In order to handle the parametric uncertainties, techniques like adaptive backstepping, tuning function are proposed as

[1]Corresponding author.

Contributed by the Dynamic Systems Division of ASME for publication in the Journal of Dynamic Systems, Measurement, and Control. Manuscript received December 9, 2016; final manuscript received June 19, 2018; published online July 23, 2018. Assoc. Editor: Manish Kumar.

solutions [31–33]. However, there are two main problems that remain in these conventional backstepping schemes: (1) the systems for which the backstepping is applicable must be in the strict-feedback form and (2) the need for the derivatives of the virtual controls. The strict-feedback form requires that the systems have a specific lower triangular structure which will restrict the applicability. And taking the derivatives of the virtual controls always results in the problem of "complexity explosion." Nevertheless, this problem can be solved by the dynamic surface control (DSC) in which low-pass filters are introduced, [34,35]. It can be seen that in the rest of this paper, after integrating the UDE-based control with the backstepping scheme, some benefits will be brought out for the backstepping to relax the strict-feedback form and solve the "complexity explosion" problem.

The main contributions of this paper are as follows:

(1) The structural constraint in the UDE-based control which appears in the literature is shown to be equivalent to the matching condition of *uncertainties and disturbances*. Therefore, the backstepping scheme is utilized to relax this limitation and the UDE-based control will be pushed to be applicable for a more general type of nonlinear systems;
(2) The intermediate system errors, which appear in the backstepping scheme, are regarded as a part of the "disturbance-like" term, which can be estimated and compensated like other disturbances by using the UDE-based control. This proposed method simplifies the way to handle the intermediate errors compared to other methods, e.g., adaptive backstepping control;
(3) The utilization of reference models which inherit from the UDE-based control design also relaxes the computation of derivatives of the virtual controls and avoids the "complexity explosion" problem in the same spirit of DSC;
(4) Compared to the conventional backstepping approach which requires the system in the strict-feedback form, the proposed method is applicable for a more general type of nonlinear systems by lumping the nonstrict-feedback form terms into the "disturbance-like" terms.

The remainder of the paper is organized as follows: In Sec. 2, the idea of the UDE-based control is introduced and the restriction named the structural constraint is analyzed. In order to relax the structural constraint, Sec. 3 reformulates the nonlinear control problem, and the UDE-based backstepping controller is proposed in Sec. 4. The stability of the closed-loop system is analyzed in Sec. 5. Furthermore, in order to evaluate the effectiveness of the proposed method, three examples, including a numerical example, a simulation study on a rotary inverted pendulum and an experimental study on a coupled water tank system are presented in Sec. 6. Section 7 presents the concluding remarks.

2 Structural Constraint or Matching Condition in the Uncertainty and Disturbance Estimator-Based Control

Similar to the formulation in Ref. [7], a single-input-single-output (SISO) linear system is considered as

$$\dot{X}(t) = (A + \Delta A)X(t) + (B + \Delta B)u(t) + D(t) \tag{1}$$

and the reference model is chosen as

$$\dot{\Omega}_r(t) = A_m\Omega_r(t) + B_m(t)x_{1r}(t) \tag{2}$$

where $X(t) = [x_1, \ldots, x_n]^{\mathrm{T}} \in \mathbb{R}^n$ is the measured system state vector, x_1 is the system output which is to be regulated, $u(t) \in \mathbb{R}$ is the control input, $D(t) \in \mathbb{R}^n$ is the external unmeasurable disturbance vector. A and B are known system matrices with suitable dimensions, and B has a full column rank. ΔA and ΔB are unknown system matrices. $\Omega_r(t) = [\omega_{1r}, \ldots, \omega_{nr}]^{\mathrm{T}} \in \mathbb{R}^n$ is the reference state vector, A_m and B_m are reference model system matrices with suitable dimensions and $x_{1r}(t) \in \mathbb{R}$ is the command signal. The reference model will make $\omega_{1r}(t)$ follow $x_{1r}(t)$, i.e., $\omega_{1r}(t) \to x_{1r}(t)$. Define the tracking error $e(t) = \Omega_r(t) - X(t)$. The control objective is to achieve the desired performance which relates to the error dynamics

$$\dot{e}(t) = (A_m + K)e(t) \tag{3}$$

where K is the error feedback gain matrix. Combining Eqs. (1)–(3) results in

$$\begin{aligned} &A_mX(t) + B_mc(t) - AX(t) - Bu(t) \\ &\quad -\Delta AX(t) - \Delta Bu(t) - D(t) = Ke(t) \end{aligned} \tag{4}$$

If the control law $u(t)$ satisfies Eq. (4), the desired error dynamics (3) can be achieved. Hence, solving Eq. (4) results in

$$\begin{aligned} u(t) &= B^+[A_mX(t) + B_mx_{1r}(t) - AX(t) - Ke(t) \\ &\quad -\Delta AX(t) - \Delta Bu(t) - D(t)] \end{aligned} \tag{5}$$

$$= B^+[A_mX(t) + B_mx_{1r}(t) - AX(t) - Ke(t) - u_d(t)] \tag{6}$$

where $B^+ = (B^{\mathrm{T}}B)^{-1}B^{\mathrm{T}}$ is the pseudoinverse of B. Since B has a full column rank, B^+ always exists. And $u_d(t) = \Delta AX(t) + \Delta Bu(t) + D(t)$ denotes the lumped "disturbance-like" term, which consists of both system uncertainties and external disturbances. Note that only under the following condition:

$$(I - BB^+)(A_mX(t) + B_mx_{1r}(t) - AX(t) - Ke(t) - u_d(t)) = 0 \tag{7}$$

Equation (5) is the accurate solution of Eq. (4). Otherwise, it is just a least square approximated solution. Equation (7) is called *the structural constraint* of the UDE-based control. From Eq. (1), it can be obtained that

$$u_d(t) = \dot{X}(t) - AX(t) - Bu(t) \tag{8}$$

In other words, the unknown "disturbance-like" term can be observed by the system states and the control signal. However, this observation cannot be used in the control law directly. Different from the TDC that adopts an estimation of this signal by using a small delay in the time domain, the UDE-based control uses a different estimation strategy by looking at this problem in the frequency domain.

Assume that $G_f(s)$ is a strictly proper low-pass filter with unity steady-state gain and zero phase shift over a broad enough bandwidth, then $u_d(t)$ can be accurately approximated as $\hat{u}_d(t)$, i.e.,

$$\hat{u}_d(t) = \left[\dot{X}(t) - AX(t) - Bu(t)\right] * \mathscr{L}^{-1}\{G_f(s)\} \tag{9}$$

where $\mathscr{L}^{-1}$ is the inverse Laplace operator and * is the convolution operator. Hence, the UDE-based controller is in the following form

$$\begin{aligned} u(t) = B^+\Bigg[&-Ax(t) + \mathscr{L}^{-1}\left\{\frac{1}{1 - G_f(s)}\right\} * (A_mx(t) \\ &+B_mx_{1r}(t) - Ke(t)) - \mathscr{L}^{-1}\left\{\frac{sG_f(s)}{1 - G_f(s)}\right\} * x(t)\Bigg] \end{aligned} \tag{10}$$

The UDE-based controller could guarantee the desired performance (3) under the condition of Eq. (7); otherwise, the behavior is not tamed. To verify under what condition that Eq. (7) will hold, a discussion is presented below.

Usually, if B is an invertible matrix, i.e., $B^+ = B^{-1}$, obviously, Eq. (7) always holds; otherwise, the selection of the reference model, the error feedback gain, the uncertainties and disturbances have some restrictions. In some applications, the system (1) is realized in the controllable companion form, i.e.,

$$A = \begin{bmatrix} 0 & I_{n-1} \\ A_n \end{bmatrix}, \quad B = \begin{bmatrix} 0 \\ b_n \end{bmatrix} \tag{11}$$

where A_n is a row vector and b_n is a scalar. Obviously, $I - BB^+ = \begin{bmatrix} I_{n-1} & 0 \\ 0 & 0 \end{bmatrix}$, in this case, in order to meet the structural constraint, the uncertainty ΔA, ΔB, and disturbance $D(t)$ should satisfy the *matching condition*, i.e.,

$$\Delta A = \begin{bmatrix} 0 \\ \Delta A_n \end{bmatrix}, \Delta B = \begin{bmatrix} 0 \\ \Delta b_n \end{bmatrix}, D(t) = \begin{bmatrix} 0 \\ d_n(t) \end{bmatrix} \tag{12}$$

where ΔA_n is a row vector and Δb_n and $d_n(t)$ are scalars. Furthermore, the selection of the reference models A_m, B_m, K is limited as

$$A_m = \begin{bmatrix} 0 & I_{n-1} \\ A_{mn} \end{bmatrix}, B_m = \begin{bmatrix} 0 \\ b_{mn} \end{bmatrix}, K = \begin{bmatrix} 0 \\ K_n \end{bmatrix} \tag{13}$$

where A_{mn} and K_n are constant row vectors, b_{mn} is a constant. This indicates that the reference model is also in the controllable companion form, and the error feedback gain matrix K should satisfy the *matching condition*, too. Under the above selections, there is

$$A_m x(t) + B_m x_{1r}(t) - Ax(t) - u_d(t) - Ke(t) = \begin{bmatrix} 0 \\ \varpi \end{bmatrix} \tag{14}$$

where ϖ can be zero or a nonzero value. Consequently, the structural constraint (7) is met. It can be seen that the structural constraint of the UDE-based control is actually equivalent to the matching condition, for which the uncertainties and disturbances should appear in the same channel with the control input.

It is reasonable that the selection of the reference models A_m and B_m is in the same controllable companion form with the system dynamics. The utilization of the reference model has two major benefits. First, a more smooth signal $\omega_{1r}(t)$ is generated to replace the command $x_{1r}(t)$. Second, the reference model could also provide the derivative information of $x_{1r}(t)$. However, the reference model can be omitted, as long as the command signal has smooth derivatives as high as the system order [25].

3 Problem Formulation

The UDE-based *robust* control can be also naturally extended to more general nonlinear systems, similar to the one described in Ref. [17]

$$\dot{X}(t) = f(X(t)) + \Delta f(X(t)) + Bu(t) + B_u(u(t)) + D(t) \tag{15}$$

where $f(\cdot) = [f_1(\cdot), \ldots, f_n(\cdot)]^{\mathrm{T}} : \mathbb{R}^n \to \mathbb{R}^n$ is a nonlinear function vector. $B_u(u(t))$ is an uncertain function vector of u. The UDE-based controller is designed in the same framework while the nonlinear uncertainties and external disturbances need to satisfy the *matching condition*, that is, $\Delta f(X(t)) = Bf_d(X(t)), B_u(u(t)) = Bb_u(t)$ and $D(t) = Bd(t)$, where $f_d(t)$, $b_u(t)$ and $d(t)$ are uncertain scalars. In order to push the UDE-based method to be applicable for a more general type of systems, how to relax the structural constraint and deal with the mismatched uncertainties and disturbances needs to be further studied.

As mentioned in Sec. 2, the structural constraint is always met while the control gain matrix B is invertible. For the first-order case, B is a scalar, and there are no more restrictions for other components. Therefore, it results in a solution to relax the structural constraint of the UDE-based control. This paper considers the control for the general nonlinear systems (15), but the uncertainties and disturbances *do not* necessarily satisfy the *matching condition*. Then, the system (15) is rewritten as the following form:

$$\begin{aligned} \dot{x}_1 &= f_1(x_1, \ldots, x_n) + \Delta f_1(x_1, \ldots, x_n) + \Delta b_1(u) + d_1 \\ \dot{x}_2 &= f_2(x_1, \ldots, x_n) + \Delta f_2(x_1, \ldots, x_n) + \Delta b_2(u) + d_2 \\ &\vdots \\ \dot{x}_n &= f_n(x_1, \ldots, x_n) + \Delta f_n(x_1, .., x_n) + \Delta b_n(u) + b_n u + d_n \end{aligned} \tag{16}$$

where $\Delta f_1(\cdot), \ldots, \Delta f_n(\cdot), \Delta b_1(\cdot), \ldots, \Delta b_n(\cdot)$ are unknown system dynamics and d_1,…,d_n are unmeasurable external disturbances. Additionally, the following reasonable assumptions are made about (16).

ASSUMPTION 1. *All the external disturbances d_i, $i = 1,\ldots,n$ are time-varying but bounded signals, i.e., $|d_i| \le C_{di}$, where the bounds, $C_{di} > 0$, are not necessary to be known.*

ASSUMPTION 2. *The reference signal x_{1r} and its derivatives $\dot{x}_{1r}, \ddot{x}_{1r}$ are smooth and bounded.*

ASSUMPTION 3. *The known system dynamics $f_i(\cdot), i = 1, \ldots, n-1$ can be rewritten as $f_i(x_1, \ldots, x_n) = \bar{f}_i(x_1, \ldots, x_i) + b_i x_{i+1} + \tilde{f}_i(x_1, \ldots, x_n)$.*

Remark 1. The assumption 3 indicates that the known system dynamics $f_i(x_1, \ldots, x_n), i = 1, \ldots, n-1$ can be split into a part in strict-feedback form $\bar{f}_i(x_1, \ldots, x_i) + b_i x_{i+1}$ and a term in nonstrict-feedback form $\tilde{f}_i(x_1, \ldots, x_n)$. The constants b_1, b_2,…,b_n are nonzero control coefficients. For the consistency, let $\bar{f}_n(x_1, \ldots, x_n) = f_n(x_1, \ldots, x_n)$.

ASSUMPTION 4. *The system dynamics $f_1(\cdot), \ldots, f_n(\cdot)$ and $\Delta f_1(\cdot), \ldots, \Delta f_n(\cdot)$ are all continuous functions and equal to zero at the origin, i.e., $f_i(0, \ldots, 0) = 0$ and $\Delta f_i(0, \ldots, 0) = 0$.*

ASSUMPTION 5. *The uncertain terms $\Delta b_i(u)$ are assumed to be Lipschitz with respect to u, and $\partial \Delta b_n(u)/\partial u \neq -b_n$.*

Consequently, the system (16) can be expressed as

$$\begin{aligned} \dot{x}_1 &= \bar{f}_1(x_1) + b_1 x_2 + \tilde{f}_1(\cdot) + \Delta f_1(\cdot) + \Delta b_1(u) + d_1 \\ \dot{x}_2 &= \bar{f}_2(x_1, x_2) + b_2 x_3 + \tilde{f}_2(\cdot) + \Delta f_2(\cdot) + \Delta b_2(u) + d_2 \\ &\vdots \\ \dot{x}_n &= \bar{f}_n(x_1, \ldots, x_n) + b_n u + \Delta f_n(\cdot) + \Delta b_n(u) + d_n \end{aligned} \tag{17}$$

For the convenience, all the functions are abbreviated as f_i, $\bar{f}_i$, $\tilde{f}_i$, Δf_i, $i = 1, \ldots, n$ in the rest of this paper. The control objective is to force the system output x_1 to track a smooth reference signal profile x_{1r}, i.e., $x_1 \to x_{1r}$ as $t \to \infty$.

It should be noted that the functions $\bar{f}_1, \ldots, \bar{f}_n$ are in the strict-feedback form for which the backstepping approach is applicable. The terms $\tilde{f}_i + \Delta f_i + \Delta b_i(u) + d_i, i = 1, \ldots, n-1$ are regarded as the mismatched uncertainties and disturbances in the strict-feedback system, while $\Delta f_n + \Delta b_n(u) + d_n$ is the matched one. The proposed method is not only applicable for the systems in the strict-feedback form but also the systems with non-strict-feedback form terms. This is much more general than the system often studied in the conventional backstepping approach.

4 Uncertainty and Disturbance Estimator-Based Backstepping Control

In order to facilitate the control design, let the variables z_1,…,z_n denote the system tracking errors, x_{2r},…,x_{nr} as the virtual controls, $\omega_{2r}, \ldots, \omega_{nr}$ as the reference signals, and y_2,…,y_n as the differences between virtual controls and reference signals. The UDE-based backstepping control design is based on the following coordinates transformation [31], $i = 2, \ldots, n$,

$$\begin{aligned} z_1 &= x_1 - x_{1r} \\ z_i &= x_i - \omega_{ir} = x_i - y_i - x_{ir} \end{aligned} \tag{18}$$

where $y_i = \omega_{ir} - x_{ir}$, $i = 2, \ldots, n$. Furthermore, a set of reference models are constructed as

$$\dot{\omega}_{ir} = -\alpha_i \omega_{ir} + \beta_i x_{ir}, \ \omega_{ir}(0) = x_{ir}(0), i = 2, \ldots, n, \tag{19}$$

where α_i and β_i are reference model parameters to be designed. It should be mentioned that the calculation for the derivatives of the virtual controls usually results in the "complexity explosion" in the conventional backstepping approach. Fortunately, with the help of the reference models in the UDE-based control design, this problem can be avoided in the same spirit of the DSC [34]. The recursive design procedure contains n steps. The design procedure begins at the first equation, which is progressively stabilized by virtual control that appears in the outer equations. The procedure terminates when the external control input is reached.

Step 1: Consider the first equation in Eq. (18). Since

$$\begin{aligned} z_1 &= x_1 - x_{1r} \\ \Rightarrow \dot{z}_1 &= \bar{f}_1 + b_1 x_2 + \tilde{f}_1 + \Delta f_1 + \Delta b_1(u) + d_1 - \dot{x}_{1r} \end{aligned} \tag{20}$$

applying $z_2 = x_2 - y_2 - x_{2r}$ results in

$$\dot{z}_1 = \bar{f}_1 + b_1 z_2 + b_1 y_2 + b_1 x_{2r} + \tilde{f}_1 + \Delta f_1 + \Delta b_1(u) + d_1 - \dot{x}_{1r} \tag{21}$$

where the virtual control x_{2r} will be derived to stabilize the scalar system (21). The virtual control x_{2r} is designed through two parts, the feedback linearization part x_{2rl} and uncertainty compensation part x_{2rd}, i.e.,

$$x_{2r} = x_{2rl} + x_{2rd} \tag{22}$$

Since z_2 and y_2 are temporal unknown for system (21), let $u_{d1} = b_1 z_2 + b_1 y_2 + \tilde{f}_1 + \Delta f_1 + \Delta b_1(u) + d_1$ as the lumped "disturbance-like" term in Eq. (21). This is different from the conventional backstepping method where z_2 remains in this step and will be eliminated by the next control step. Selecting

$$x_{2rl} = \left(-k_1 z_1 - \bar{f}_1 + \dot{x}_{1r}\right) b_1^{-1} \tag{23}$$

where $k_1 > 0$ and

$$x_{2rd} = -\left(b_1 z_2 + b_1 y_2 + \tilde{f}_1 + \Delta f_1 + \Delta b_1(u) + d_1\right) b_1^{-1} = -u_{d1} b_1^{-1} \tag{24}$$

the closed-loop system becomes

$$\dot{z}_1 = -k_1 z_1 \tag{25}$$

Since $k_1 > 0$, the system state z_1 is exponentially stable, $z_1 = e^{-k_1 t} z_1(0)$, i.e., $z_1 \to 0$ as $t \to \infty$. However, u_{d1} is unknown and cannot be used directly in Eq. (24). The disturbance compensation should be redesigned. Substituting Eqs. (22) and (23) into the system (21) yields

$$\dot{z}_1 = -k_1 z_1 + b_1 x_{2rd} + u_{d1} \tag{26}$$

Solving u_{d1} leads to

$$u_{d1} = \dot{z}_1 + k_1 z_1 - b_1 x_{2rd} \tag{27}$$

which indicates that u_{d1} can be observed by the signals z_1, x_{2rd}. Using a proper low-pass filter $G_{f1}(s)$, which has unity steady-state gain and zero phase shift in the spectrum of u_{d1}, the disturbance can be estimated by

$$\hat{u}_{d1} = \mathscr{L}^{-1}\{G_{f1}(s)\} * (\dot{z}_1 + k_1 z_1 - b_1 x_{2rd}) \tag{28}$$

Then, the uncertainty compensation is rewritten as

$$\begin{aligned} x_{2rd} &= -\hat{u}_{d1} b_1^{-1} \\ &= -\mathscr{L}^{-1}\{G_{f1}(s)\} * (\dot{z}_1 + k_1 z_1 - b_1 x_{2rd}) b_1^{-1} \end{aligned} \tag{29}$$

Solving x_{2rd} yields

$$x_{2rd} = -\mathscr{L}^{-1}\left\{\frac{G_{f1}}{1 - G_{f1}}\right\} * (\dot{z}_1 + k_1 z_1) b_1^{-1} \tag{30}$$

It can be seen that the estimation of u_{d1} can be calculated by

$$\hat{u}_{d1} = \mathscr{L}^{-1}\left\{\frac{G_{f1}}{1 - G_{f1}}\right\} * (\dot{z}_1 + k_1 z_1) \tag{31}$$

Hence, the virtual control (22) for (21) can be designed as

$$\begin{aligned} x_{2r} = &\left[-k_1 z_1 - \bar{f}_1 + \dot{x}_{1r}\right] b_1^{-1} \\ &-\mathscr{L}^{-1}\left\{\frac{G_{f1}}{1 - G_{f1}}\right\} * (\dot{z}_1 + k_1 z_1) b_1^{-1} \end{aligned} \tag{32}$$

Consequently, substituting Eqs. (22), (23), and (29) into Eq. (21) results in the closed-loop system

$$\dot{z}_1 = -k_1 z_1 + (u_{d1} - \hat{u}_{d1}) \tag{33}$$

Step i: ($i = 2, \ldots, n-1$) Consider the ith equation in Eq. (18)

$$\begin{aligned} z_i &= x_i - \omega_{ir} \\ \Rightarrow \dot{z}_i &= \bar{f}_i + b_i x_{i+1} + \tilde{f}_i + \Delta f_i + \Delta b_i(u) + d_i - \dot{\omega}_{ir} \end{aligned} \tag{34}$$

Applying $z_i = x_i - y_i - x_{ir}$ results in

$$\begin{aligned} \dot{z}_i = &\bar{f}_i + b_i z_{i+1} + b_i y_{i+1} + b_i x_{(i+1)r} + \tilde{f}_i \\ &+\Delta f_i + \Delta b_i(u) + d_i - \dot{\omega}_{ir} \end{aligned} \tag{35}$$

Similarly, since z_{i+1} and y_{i+1} are unknown for system (35), let $u_{di} = b_i z_{i+1} + b_i y_{i+1} + \tilde{f}_i + \Delta f_i + \Delta b_i(u) + d_i$ be the lumped "disturbance-like" term and follow the same procedure with step 1. The virtual control $x_{(i+1)r}$ is obtained as

$$x_{(i+1)r} = x_{(i+1)rl} + x_{(i+1)rd} \tag{36}$$

the feedback linearization part is designed as

$$x_{(i+1)rl} = \left(-k_i z_i - \bar{f}_i + \dot{\omega}_{ir}\right) b_i^{-1} \tag{37}$$

where $k_i > 0$ and the uncertainty compensation part is designed as

$$x_{(i+1)rd} = -\mathscr{L}^{-1}\left\{\frac{G_{fi}}{1 - G_{fi}}\right\} * (\dot{z}_i + k_i z_i) b_i^{-1} \tag{38}$$

Combining the reference models (19), the virtual control is

$$\begin{aligned} x_{(i+1)r} = &\left[-k_i z_i - \bar{f}_i + \dot{\omega}_{ir}\right] b_i^{-1} \\ &-\mathscr{L}^{-1}\left\{\frac{G_{fi}}{1 - G_{fi}}\right\} * (\dot{z}_i + k_i z_i) b_i^{-1} \\ = &\left[-k_i z_i - \bar{f}_i - \alpha_i \omega_{ir} + \beta_i x_{ir}\right] b_i^{-1} \end{aligned} \tag{39}$$

$$-\mathscr{L}^{-1}\left\{\frac{G_{fi}}{1 - G_{fi}}\right\} * (\dot{z}_i + k_i z_i) b_i^{-1} \tag{40}$$

Consequently, the resulting closed-loop system is

$$\dot{z}_i = -k_i z_i + (u_{di} - \hat{u}_{di}) \tag{41}$$

Step n: Consider the last equation in Eq. (18),

$$\begin{aligned} z_n &= x_n - \omega_{nr} \\ \Rightarrow \dot{z}_n &= \bar{f}_n + b_n u + \Delta f_n + \Delta b_n(u) + d_n - \dot{\omega}_{nr} \end{aligned} \tag{42}$$

Let the lumped "disturbance-like" term be $u_{dn} = \Delta f_n + \Delta b_n(u) + d_n$ and follow the same procedures, the control input is obtained as

$$u = \left[-k_n z_n - \bar{f}_n + \dot{\omega}_{nr}\right] b_n^{-1} - \mathcal{L}^{-1}\left\{\frac{G_{fn}}{1 - G_{fn}}\right\} * (\dot{z}_n + k_n z_n) b_n^{-1} \tag{43}$$

$$= \left[-k_n z_n - \bar{f}_n - \alpha_n \omega_{nr} + \beta_n x_{nr}\right] b_n^{-1} - \mathcal{L}^{-1}\left\{\frac{G_{fn}}{1 - G_{fn}}\right\} * (\dot{z}_n + k_n z_n) b_n^{-1} \tag{44}$$

where $k_n > 0$. At last, the resulting closed-loop system is obtained as

$$\dot{z}_n = -k_n z_n + (u_{dn} - \hat{u}_{dn}) \tag{45}$$

The UDE-based backstepping algorithm is then summarized in the Algorithm 1 and its structure is also illustrated in Fig. 1. It can be obtained that the closed-loop system is as follows:

$$\begin{aligned} \dot{z}_1 &= -k_1 z_1 + \tilde{u}_{d1} \\ \dot{z}_2 &= -k_2 z_2 + \tilde{u}_{d2} \\ &\vdots \\ \dot{z}_n &= -k_n z_n + \tilde{u}_{dn} \end{aligned} \tag{46}$$

where $k_i,\ k_n > 0,\ \tilde{u}_{di} = u_{di} - \hat{u}_{di},\ u_{di} = b_i z_{i+1} + b_i y_{i+1} + \tilde{f}_i + \Delta f_i + \Delta b_i(u) + d_i,\ i = 1, 2, \ldots, n-1$ and $\tilde{u}_{dn} = u_{dn} - \hat{u}_{dn}$, $u_{dn} = \Delta f_n + \Delta b_n(u) + d_n$. It can be seen that the performance of the closed-loop system is determined by the uncertainties and disturbances estimation errors, $\tilde{u}_{di}$.

Algorithm 1 UDE-based backstepping control for the nonlinear system (16)

1: $z_1 = x_1 - x_{1r}$
2: $x_{2r} = \left[-k_1 z_1 - \bar{f}_1 + \dot{x}_{1r}\right] b_1^{-1} - \mathcal{L}^{-1}\left\{\frac{G_{f1}}{1 - G_{f1}}\right\} * (\dot{z}_1 + k_1 z_1) b_1^{-1}$
3: $\dot{\omega}_{2r} = -\alpha_2 \omega_{2r} + \beta_2 x_{2r},\ \omega_{2r}(0) = x_{2r}(0)$
4: $z_2 = x_2 - \omega_{2r}$
5: **for** $i = 2$ to $n-1$ **do**
6: $x_{(i+1)r} = \left[-k_i z_i - \bar{f}_i - \alpha_i \omega_{ir} + \beta_i x_{ir}\right] b_i^{-1} - \mathcal{L}^{-1}\left\{\frac{G_{fi}}{1 - G_{fi}}\right\} * (\dot{z}_i + k_i z_i) b_i^{-1}$
7: $\dot{\omega}_{(i+1)r} = -\alpha_{i+1} \omega_{(i+1)r} + \beta_{i+1} x_{(i+1)r},\ \omega_{(i+1)r}(0) = x_{(i+1)r}(0)$
8: $z_{i+1} = x_{i+1} - \omega_{(i+1)r}$
9: **end for**
10: $u = \left[-k_n z_n - \bar{f}_n - \alpha_n \omega_{nr} + \beta_n x_{nr}\right] b_n^{-1} - \mathcal{L}^{-1}\left\{\frac{G_{fn}}{1 - G_{fn}}\right\} * (\dot{z}_n + k_n z_n) b_n^{-1}$

5 Stability Analysis of the Closed-Loop System

The following theorem shows the stability and control performance of the closed-loop system.

THEOREM 1. *(Uniformly ultimate bounded stability) Consider the nth-order nonlinear system (16) which satisfies assumptions 1–5. The initial values are chosen to make V(0), which is defined in Eq. (55), sufficiently close to the origin. After applying the Algorithm 1, it results in a series of virtual controls x_{2r}, x_{3r}, x_{nr} and the control input u.*

Then

(i) *all signals in the closed-loop system, $x_1, \ldots, s, x_n, x_{2r}, \ldots, x_{nr}$, $z_1, \ldots, z_n, y_2, \ldots, y_n$ are bounded.*
(ii) *the system tracking error $|x_1 - x_{1r}|$ can be adjusted within an arbitrarily small compact set by changing the control parameters.*

Proof. First, define the vectors $X = [x_1, \ldots, x_n]^{\mathrm{T}}$, $Y = [y_2, \ldots, y_n]^{\mathrm{T}}$, $Z = [z_1, \ldots, z_n]^{\mathrm{T}}$, and the compact sets $\Omega_x = \{X : ||X||_2^2 \le p_1\}$, $\Omega_y = \left\{Y : ||Y||_2^2 \le 2p_2\right\}$ and $\Omega_z = \left\{Z : ||Z||_2^2 \le 2p_3\right\}$, where p_1, p_2, p_3 are arbitrary positive constants, $\Omega_x, \Omega_y, \Omega_z$ are local neighborhoods of the origin in the X, Y, Z space, respectively.

By using the Algorithm 1, the resulting closed-loop system is (46). According to the Young's inequality, there is

$$\begin{aligned} z_i \dot{z}_i &= -k_i z_i^2 + z_i \tilde{u}_{di} \le -k_i z_i^2 + \frac{z_i^2}{2\varepsilon} + \frac{\varepsilon \tilde{u}_{di}^2}{2} \\ &= -\bar{k}_i z_i^2 + \frac{\varepsilon \tilde{u}_{di}^2}{2} \end{aligned} \tag{47}$$

where $\varepsilon > 0$, and $\bar{k}_i = k_i - 1/(2\varepsilon) > 0$. Consider the following Lyapunov function candidate

$$V_z = \frac{1}{2} \sum_{i=1}^{n} z_i^2 \tag{48}$$

Taking the derivative of both sides of the above equation leads to

$$\dot{V}_z = \sum_{i=1}^{n} z_i \dot{z}_i \le -\sum_{i=1}^{n} \bar{k}_i z_i^2 + \sum_{i=1}^{n} \frac{\varepsilon \tilde{u}_{di}^2}{2} \le -C_z V_z + \sum_{i=1}^{n} \frac{\varepsilon \tilde{u}_{di}^2}{2} \tag{49}$$

where $C_z = \min\left\{(\bar{k}_i/2), i = 1, \ldots, n\right\}$, and the functions $\tilde{u}_{di} = u_{di} - \hat{u}_{di}$ are continuous functions of $x_1, \ldots, x_n, z_1, \ldots, z_n, y_2, \ldots, y_n$ and $d_1, \ldots, d_n, x_{1r}, \dot{x}_{1r}, \ddot{x}_{1r}$. According to Eq. (19), there is

$$\dot{y}_i = -\alpha_i y_i + (\beta_i - \alpha_i) x_{ir} - \dot{x}_{ir} \tag{50}$$

thus

$$|\dot{y}_i + \alpha_i y_i| \le \xi_i \tag{51}$$

where ξ_i is a continuous function of $x_1, \ldots, x_i, z_1, \ldots, z_i, y_2, \ldots, y_i$ and $d_1, \ldots, d_i, x_{1r}, \dot{x}_{1r}, \ddot{x}_{1r}$. Furthermore

$$\begin{aligned} \dot{y}_i y_i &\le -\alpha_i y_i^2 + |y_i| \xi_i \\ &\le -\alpha_i y_i^2 + \frac{y_i^2}{2\varepsilon} + \frac{\varepsilon \xi_i^2}{2} \\ &= -\bar{\alpha}_i y_i^2 + \frac{\varepsilon \xi_i^2}{2} \end{aligned} \tag{52}$$

where $\bar{\alpha}_i = \alpha_i - 1/(2\varepsilon) > 0$. Next, considering the Lyapunov function candidate

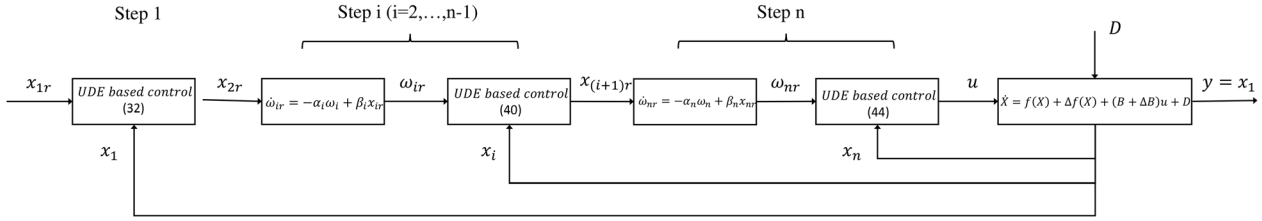

Fig. 1 Structure of the UDE-based backstepping control

$$V_y = \frac{1}{2}\sum_{i=2}^{n} y_i^2 \tag{53}$$

there is

$$\dot{V}_y = \sum_{i=2}^{n} y_i \dot{y}_i = -\sum_{i=2}^{n} \bar{\alpha}_i y_i^2 + \sum_{i=2}^{n} \frac{\varepsilon \xi_i^2}{2} \le -C_y V_y + \sum_{i=2}^{n} \frac{\varepsilon \xi_i^2}{2} \tag{54}$$

where $C_y = \min\{(\bar{\alpha}_i/2), i = 2, \ldots, n\}$. Defining the composite Lyapunov function candidate

$$V = V_z + V_y \tag{55}$$

thus

$$\dot{V} = \dot{V}_z + \dot{V}_y \le -C_z V_z - C_y V_y + \sum_{i=1}^{n} \frac{\varepsilon \tilde{u}_{di}^2}{2} + \sum_{i=2}^{n} \frac{\varepsilon \xi_i^2}{2} \tag{56}$$

Under assumptions 1 and 2, there is $(d_1, d_2, d_3) \in \mathcal{N}_d \subset \mathbb{R}^3$, $(x_{1r}, \dot{x}_{1r}, \ddot{x}_{1r}) \in \mathcal{N}_r \subset \mathbb{R}^3$. Considering the compact set $\Omega = \Omega_x \times \Omega_z \times \Omega_y \times \mathcal{N}_d \times \mathcal{N}_r$, with assumption 5, while $|\Delta b_i|$ are small enough, the functions $\tilde{u}_{di}$ are continuous inside the compact set Ω. Henceforth, there exists a maximum value for $(1/2)\sum_{i=1}^{n} \tilde{u}_{di}^2$, say $M_1 > 0$. Next, consider the functions ξ_i are also continuous inside the compact set Ω, so that there exists a maximum value for $(1/2)\sum_{i=2}^{n} \xi_i^2$, say $M_2 > 0$. Therefore, Eq. (56) can be rewritten as

$$\dot{V} \le -\mu V + \varepsilon\zeta \tag{57}$$

where $\mu = \min\{C_z, C_y\} > 0$ and $\zeta = M_1 + M_2 > 0$. Solving the inequality Eq. (57) gives

$$0 \le V(t) \le V(0)e^{-\mu t} + \frac{\varepsilon\zeta}{\mu}(1 - e^{-\mu t}) \quad t \ge 0 \tag{58}$$

Let $p = p_1 + p_2 + p_3$, if the control parameters, $k_1, \ldots, k_n, \alpha_2, \beta_2, \ldots, \alpha_n, \beta_n$, are chosen to satisfy $p > (\varepsilon\zeta/\mu)$ and from Eq. (57) there is $\dot{V} < 0$ on $V \ge p$. Furthermore, if the initial condition satisfies that $V(0) \le p - (\varepsilon\zeta/\mu)$, there is $V(t) \le p$ for all $t \ge 0$. As shown in Fig. 2, the compact set Ω is an invariant set. $\varepsilon > 0$ is a tuning coefficient, which determines the size of invariant set Ω. The smaller ε is, the smaller invariant set Ω is. No matter how small ε is, one can choose the parameters to satisfy that $k_i > 1/(2\varepsilon), i = 1, .., n, \alpha_j > 1/(2\varepsilon), j = 2, \ldots, n$ so that $\dot{V} \le -\mu V + \varepsilon\zeta$ can be guaranteed. Then all signals in the closed-loop system can converge to a small region.

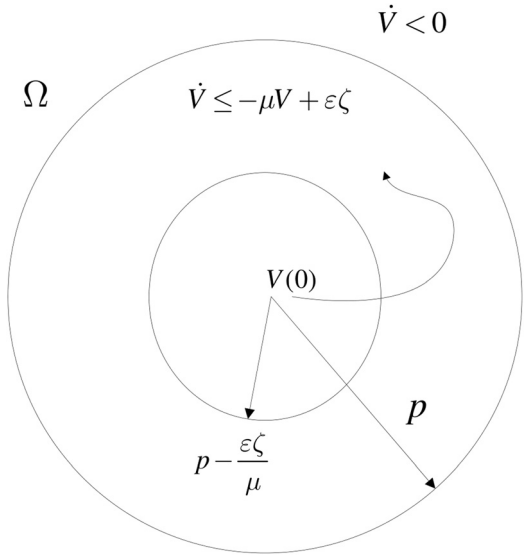

Fig. 2 Compact invariant set

Hence, the error signals $z_1, \ldots z_n, y_2, \ldots, y_n$ are all bounded. Due to the boundedness of $d_1, \ldots, d_n, x_{1r}$ and $u_{di} = z_{i+1} + y_{i+1} + d_i$, it can be concluded that the lumped uncertainties u_{d1},…,u_{dn} are also bounded. After applying the stable filters $G_{fi}(s)$, it leads to the boundedness of the virtual controls x_{2r},…, x_n and system states x_1,…, x_n. Consequently: (*i*) the signals x_1,…, x_n, x_{2r},…, x_{nr}, z_1,., z_n, y_2,…, y_n are bounded.

From (58), as $t \to \infty$, $V(t) < \varepsilon\zeta/\mu$, then $|z_1| = |x_1 - x_{1r}| < \sqrt{\varepsilon\zeta/\mu}$. Since $\mu = \min\{(k_i/2) - (1/4\varepsilon), (\alpha_j/2) - (1/4\varepsilon)\}, i = 1, \ldots, n, j = 2, \ldots, n$, $\sqrt{\varepsilon\zeta/\mu} = 2\varepsilon\sqrt{\zeta/(\min\{2\varepsilon k_i - 1, 2\varepsilon\alpha_j - 1\})}$. Increasing the parameters $k_1, \ldots, k_n, \alpha_2, \ldots, \alpha_n$ will result in a greater denominator, a smaller error bound. On the other hand, $\zeta = M_1 + M_2$, M_1 depends on the estimation error of the lumped uncertainties, $\tilde{u}_{di}$, which can be adjusted by the filters $G_{fi}(s)$ in the UDE [12]. The second term M_2 is determined by the continuous function ξ_i on Ω. Increasing $k_1, \ldots, k_n, \alpha_2, \ldots, \alpha_n$ will make M_2 greater. Therefore, there exists a tradeoff when tuning the parameters $k_1, \ldots, k_n, \alpha_2, \ldots, \alpha_n$. To a summary, in order to decrease the bound of $|z_1|$, one can properly adjust the control parameters $k_1, \ldots, k_n, \alpha_2, \ldots, \alpha_n$, and design $G_{fi}(s)$. Therefore, (*ii*) the bound for $|z_1|$ can be decreased to arbitrarily small. This ends the proof.

6 Validations

To validate the proposed control strategy, a second-order numerical example, a simulation study based on a rotary inverted pendulum, and an experimental study based on a coupled water tank system are carried out in this section.

6.1 Simulation Study: A Second-Order System. Consider the following second-order nonlinear system:

$$\dot{x}_1 = x_1^2 + x_2 + 0.2e^{x_1} + 0.25x_2 \sin u + d_1 \tag{59}$$

$$\dot{x}_2 = -x_1 x_2^2 + \cos u + u + d_2 \tag{60}$$

where x_1 is the regulated variable and u is the control input. The external disturbances are $d_1 = 0.5 \sin 4\pi t$, $d_2 = 0.15 \sin 20\pi t$, and the desired reference signal is $x_{1r} = \sin(2\pi/3)t$. In this system, the lumped "disturbance-like" terms are $u_{d1} = z_2 + y_2 + x_1^2 + 0.2e^{x_1} + 0.25x_2 \sin u + d_1$ and $u_{d2} = -x_1 x_2^2 + \cos u + d_2$. According to the Algorithm 1, the control design is provided as follows:

Step 1. Let $z_1 = x_1 - x_{1r}$, the virtual control is obtained as

$$x_{2r} = -k_1 z_1 + \dot{x}_{1r} - \mathcal{L}^{-1}\left\{\frac{G_{f1}(s)}{1 - G_{f1}(s)}\right\} * (\dot{z}_1 + k_1 z_1)$$

The filter used in the controller is $G_{f1}(s) = 1/(\tau_1 s + 1)$, which is a first-order low-pass filter with a bandwidth $1/\tau_1$. Then, the reference model is used to generate the reference signal for the next step, $\dot{\omega}_{2r} = -\alpha_2\omega_{2r} + \beta_2 x_{2r}, \omega_{2r}(0) = x_{2r}(0) = 0$, where $\alpha_2 = \beta_2 = B_r$. Here, B_r represents the bandwidth of the reference model.

Step 2. Let $z_2 = x_2 - \omega_{2r}$, the control input is

$$u = -k_2 z_2 - \alpha_2\omega_{2r} + \beta_2 x_{2r} - \mathcal{L}^{-1}\left\{\frac{G_{f2}(s)}{1 - G_{f2}(s)}\right\} * (\dot{z}_2 + k_2 z_2)$$

where $G_{f2}(s) = 1/(\tau_2 s + 1)$ is a first-order low-pass filter with a bandwidth $1/\tau_2$.

Figure 3 shows the control results while $k_1 = 15$, $k_2 = 80$, $\alpha_2 = \beta_2 = 100$, and $\tau_1 = \tau_2 = 0.01$. The successful tracking for x_{1r} and x_{2r} are shown in Figs. 3(*a*) and 3(*b*). Figures 3(*c*) and 3(*d*)

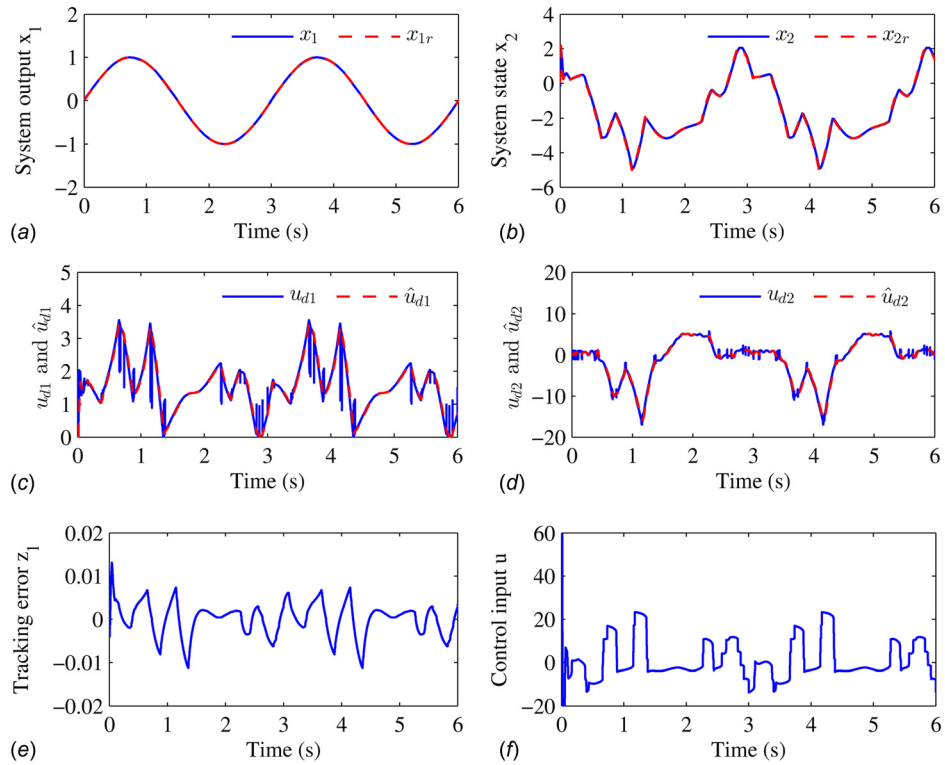

Fig. 3 Numerical control results of the systems (59) and (60)

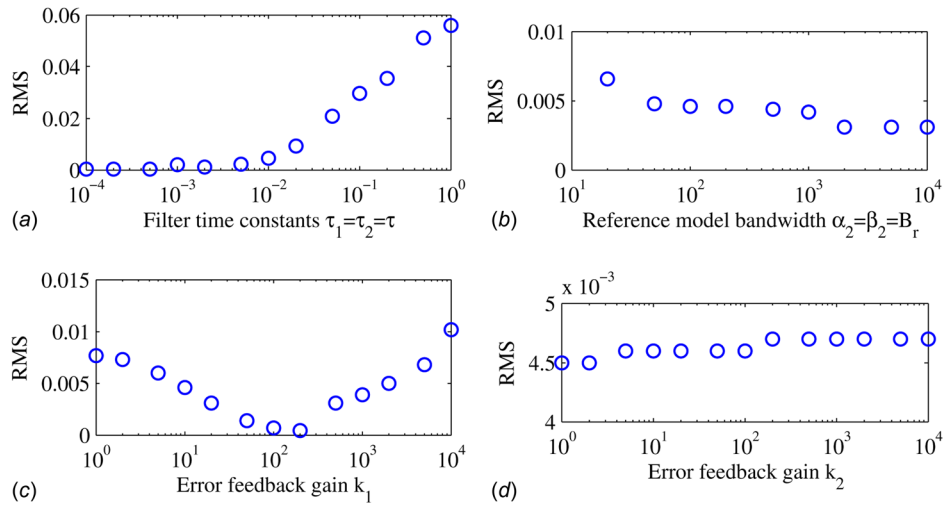

Fig. 4 Effect of different parameters

show that both u_{d1} and u_{d2} can be well estimated. In Fig. 3(*e*), the root-mean-square (RMS) of the tracking error during 3–6 s is calculated as 0.0046, which illustrates a good tracking performance. The control input u is shown in Fig. 3(*f*).

Figure 4 shows the effect of different parameters, where the RMS during the steady-state 3–6 s is used as a criterion. The reference model bandwidth is $\alpha_2 = \beta_2 = B_r$, and the time constants for the UDE filters are $\tau_1 = \tau_2 = \tau$. The parameters are chosen as follows:

(1) Figure 4(*a*), $k_1 = 15$, $k_2 = 80$, $B_r = 100$, $\tau \in [0.0001, 1]$.
(2) Figure 4(*b*), $k_1 = 15$, $k_2 = 80$, $\tau = 0.01$, $B_r \in [10, 10000]$.

Table 1 Selection of parameters

Parameters	Spectrum of u_{di}	Reference models α_i, β_i	UDE filter $G_{fi} = \dfrac{1}{\tau_i s + 1}$	Error feedback gain k_i
$i = 1$	[0, 2 Hz]	N/A	$\tau_1 < \dfrac{1}{2\pi \times 2}$	$k_1 > 2\pi \times 2$
$i = 2$	[0, 10 Hz]	$\alpha_2 = \beta_2 = B_r \gg \dfrac{2\pi}{3}$	$\tau_2 < \dfrac{1}{2\pi \times 10}$	$k_2 > 2\pi \times 10$ and $k_2 \geq k_1$

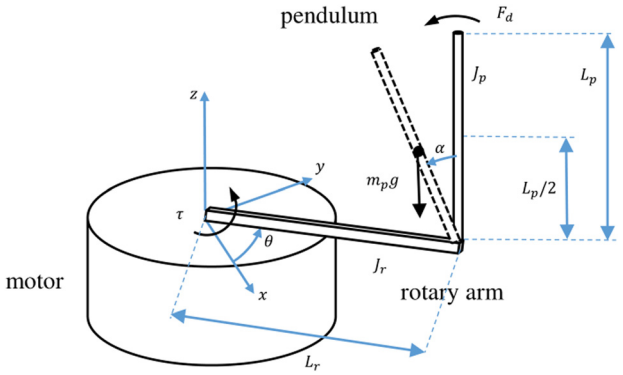

Fig. 5 A rotary inverted pendulum

(3) Figure 4(*c*), $k_2 = 80$, $B_r = 100$, $\tau = 0.01$, $k_1 \in [1, 10000]$.
(4) Figure 4(*d*), $k_1 = 15$, $B_r = 100$, $\tau = 0.01$, $k_2 \in [1, 10000]$.

The tuning guideline for the parameters can be concluded from the above results. For the time constants of the UDE filters, τ_i determines the estimation accuracy of u_{di}. A smaller τ_i guarantees a better estimation of u_{di}. In practice, τ_i, $i = 1,2$ can be chosen the same with τ. And τ should be as small as possible, which is only limited by the sampling time in hardware. The reference model bandwidth B_r should be chosen wide enough to provide a good approximation between ω_{2r} and x_{2r}. An insufficient large B_r can lead to a large intermediate system error y_2 in u_{d1}; thus, the tracking performance may degrade. The error feedback gain k_1 determines the tracking error z_1 directly. As shown in Fig. 4(*c*), there is a tradeoff while selecting k_1. k_1 cannot be too large, since it may cause instability. A proper large k_1 is needed to obtain a good tracking performance. Figure 4(*d*) shows that k_2 does not affect z_1 explicitly. The effect of k_2 only appears in z_2, which is lumped in u_{d1} and compensated through the UDE-based control. Moreover, it is reasonable to choose $k_2 \geq k_1$ to make the inner loop faster than the outer loop in Fig. 1.

In this example, the reference signal x_{1r} is at $(1/3)$Hz, d_1 at 2 Hz, and d_2 at 10 Hz. The virtual control x_{2r} is also at $(1/3)$Hz. Furthermore, the spectra of u_{d1} and u_{d2} can be estimated as [0, 2 Hz] and [0, 10 Hz], respectively. Table 1 summarizes the parameter tuning guideline of this example. The reference model bandwidth $B_r = 100$ is much greater than $(2\pi/3)$ so that ω_{2r} can well approximate x_{2r}, and the intermediate system error y_2 does not contribute to u_{d1} too much. The time constants of the two UDE filters are selected as $\tau_1 = \tau_2 = 0.01 < 1/(20\pi)$; henceforth, both u_{d1} and u_{d2} can be well estimated. According to (46), $z_1 = \mathcal{L}^{-1}\{1/(s+k_1)\} * \tilde{u}_{d1}$ and $z_2 = \mathcal{L}^{-1}\{1/(s+k_2)\} * \tilde{u}_{d2}$. One can choose $k_1 = 15 > 4\pi$ and $k_2 = 80 > 20\pi$ so that z_1 and z_2 can be reduced to a small region. It is worth noticing that the above tuning procedure only requires the spectrum information of u_{d1} and u_{d2}.

6.2 Simulation Study: Robust Stabilization of a Rotary Inverted Pendulum. It can be seen that in Fig. 5, a rotary inverted pendulum system is composed of a pendulum attached to the end of a rotary arm controlled by a motor.

As a popular mechanical system, its model can be referred to Ref. [36] and the system parameters are listed in Table 2. The system dynamics is expressed as

$$a_{11}\ddot{\alpha} - a_{12}\cos(\alpha)\ddot{\theta} = b_{11}\sin\alpha + b_{12}\dot{\alpha} + F_d \tag{61}$$

$$-a_{21}\cos(\alpha)\ddot{\alpha} + a_{22}\ddot{\theta} = b_{21}\dot{\alpha}^2\sin\alpha + b_{22}\dot{\theta} + b_u V_m \tag{62}$$

where α and θ are the pendulum angle and rotary arm angle, respectively; F_d is the external torque disturbance applied on the pendulum, and V_m is the input motor voltage. The control objective is to maintain the pendulum at the upright position, while the rotary arm angle is stabilized.

In order to stabilize the pendulum, the following coordinate transformation is applied to obtain a system in cascaded form with mismatched uncertainties and disturbances:

$$x_1 = \alpha + \lambda\left(a_{11}\dot{\alpha} - a_{12}\cos(\alpha)\dot{\theta}\right) \tag{63}$$

$$x_2 = \dot{\alpha} \tag{64}$$

where $\lambda > 0$ is a constant. After taking the derivatives and combining with Eqs. (61) and (62), it results in the following cascaded systems (65) and (66), which is in a non-strict-feedback form as (17).

The term $(\lambda a_{12}\dot{\theta}\sin\alpha)x_2 + \lambda(b_{11}\sin\alpha + F_d)$ in Eq. (65) is the mismatched uncertainty and disturbance for the system. Since $F_\alpha(\alpha, \dot{\theta}, x_2)$ is assumed to be unknown, it plays the role of matched uncertainty and disturbance. In this system, the lumped "disturbance-like" terms are $u_{d1} = (1 + \lambda b_{12})(z_2 + y_2) + (\lambda a_{12}\dot{\theta}\sin\alpha)x_2 + \lambda(b_{11}\sin\alpha + F_d)$ and $u_{d2} = F_\alpha(\alpha, \dot{\theta}, x_2)$. Furthermore, the external disturbance torque is $F_d = -0.25\,\mathrm{N}\cdot\mathrm{m}$ during 4–4.2 s and $F_d = 0.3\,\mathrm{N}\cdot\mathrm{m}$ during 8–8.2 s. The initial states of α and θ are 5 deg and 0 deg, respectively. The control objective is to stabilize $x_1 \to 0$. This implies that $\alpha \to 0$ and $\dot{\theta} \to 0$.

$$\dot{x}_1 = (1 + \lambda b_{12})x_2 + (\lambda a_{12}\dot{\theta}\sin\alpha)x_2 + \lambda(b_{11}\sin\alpha + F_d) \tag{65}$$

$$\dot{x}_2 = F_\alpha(\alpha, \dot{\theta}, x_2) + b_\alpha V_m \tag{66}$$

$$F_\alpha(\alpha, \dot{\theta}, x_2) = \frac{a_{22}}{\det(D(\alpha))}(b_{11}\sin\alpha + b_{12}x_2 + F_d) + \frac{a_{12}\cos\alpha}{\det(D(\alpha))}\left(b_{21}x_2^2\sin\alpha + b_{22}\dot{\theta}\right),$$

$$b_\alpha = \frac{a_{12}b_u\cos\alpha}{\det(D(\alpha))},\ \det(D(\alpha)) = a_{11}a_{22} - a_{12}a_{21}\cos^2\alpha$$

The stabilization is a special case of the reference tracking problem, that is, $x_{1r} = \dot{x}_{1r} = 0$. The UDE-based backstepping controller is designed by two successive steps according to the Algorithm 1.

Step 1. Let $z_1 = x_1$, the virtual control is

$$x_{2r} = (1 + \lambda b_{12})^{-1}\left[-k_1 z_1 - \mathcal{L}^{-1}\left\{\frac{G_{f1}(s)}{1 - G_{f1}(s)}\right\} * (\dot{z}_1 + k_1 z_1)\right]$$

where $\lambda = 4$, $k_1 = 4$. The filter used in the controller is $G_{f1}(s) = 1/(0.01s + 1)$, which is a first-order low-pass filter with a cut-off frequency at around 100 rad/s. Then, the reference model is used to generate the reference signal for the next step, $\dot{\omega}_{2r} = -\alpha_2\omega_{2r} + \beta_2 x_{2r}, \omega_{2r}(0) = x_{2r}(0) = 0$, where $\alpha_2 = \beta_2 = 100$.

Table 2 Parameters of the rotary inverted pendulum [36]

Parameters	a_{11}	a_{12}	a_{21}	a_{22}	b_u
Values	$0.0330\,\mathrm{kg}\cdot\mathrm{m}^2$	$0.0135\,\mathrm{kg}\cdot\mathrm{m}^2$	$0.0135\,\mathrm{kg}\cdot\mathrm{m}^2$	$0.0079\,\mathrm{kg}\cdot\mathrm{m}^2$	$0.0256\,\mathrm{N}\cdot\mathrm{m/V}$
Parameters	b_{11}	b_{12}	b_{21}	b_{22}	
Values	$0.7450\,\mathrm{kg}\cdot\mathrm{m}^2/\mathrm{s}^2$	$-0.0024\,\mathrm{N}\cdot\mathrm{m}\cdot\mathrm{s/rad}$	$-0.0135\,\mathrm{kg}\cdot\mathrm{m}^2$	$-0.0052\,\mathrm{N}\cdot\mathrm{m}\cdot\mathrm{s/rad}$	

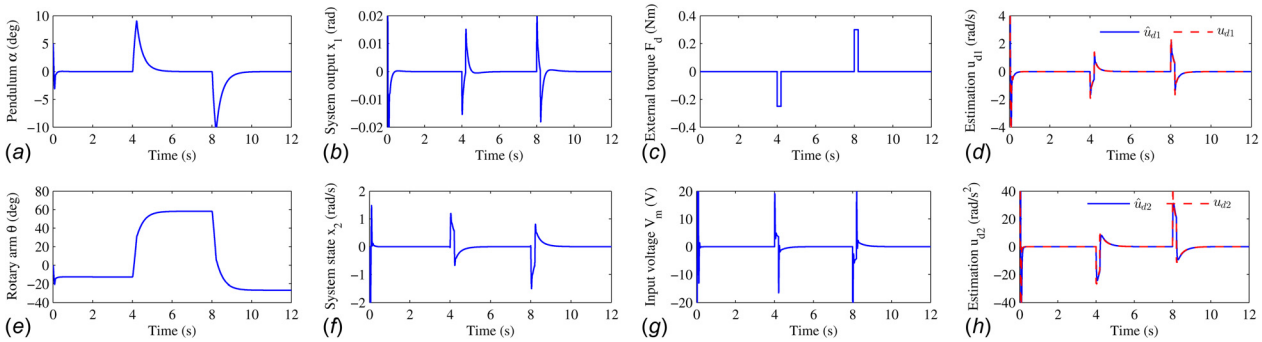

Fig. 6 Stabilization of a rotary inverted pendulum

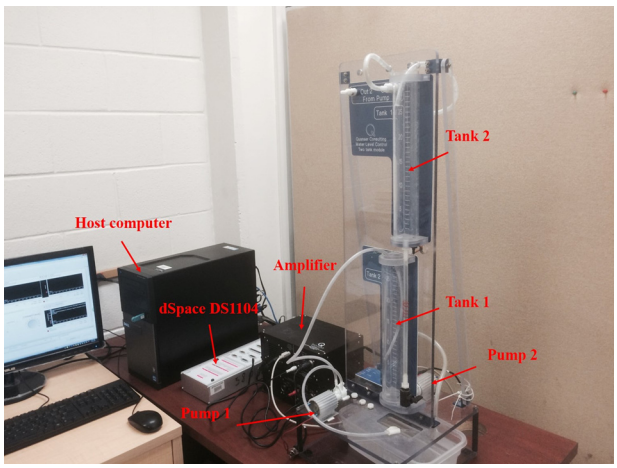

Fig. 7 A coupled water tank system

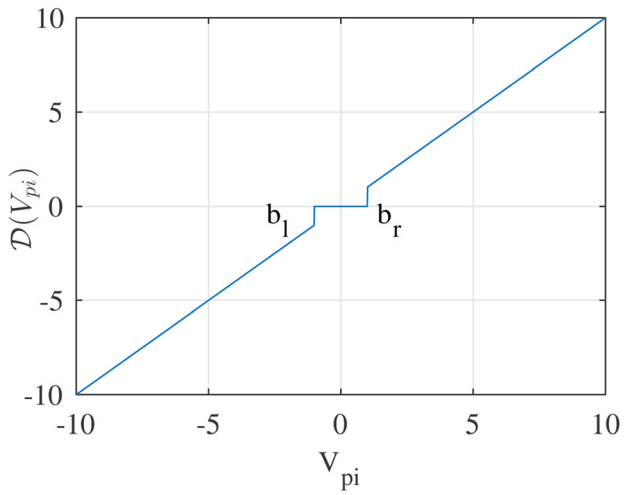

Fig. 8 Dead zone of the pump voltage

Step 2. Let $z_2 = x_2 - \omega_{2r}$, the control input is

$$V_m = b_\alpha^{-1}\left[-k_2 z_2 - \alpha_2 \omega_{2r} + \beta_2 x_{2r} - \mathscr{L}^{-1}\left\{\frac{G_{f2}(s)}{1-G_{f2}(s)}\right\} * (\dot{z}_2 + k_2 z_2)\right]$$

where $k_2 = 8$ and $G_{f2}(s) = 1/(0.02s + 1)$.

The simulation results are presented in Fig. 6. It can be seen that the pendulum angle is successfully stabilized to 0 deg, which is the upright position in Fig. 6(*a*). The rotary arm angle is convergent to around -12 deg when it arrives at the steady-state during 2–4 s, 58 deg during 6–8 s and -27 deg during 10–12 s, as shown in Fig. 6(*e*). This illustrates that the rotary arm angle is stabilized and converges to some arbitrary constants to make $\dot{\theta} = 0$. Hence, the transformed coordinates x_1, x_2 converge to 0, as shown in Figs. 6(*b*) and 6(*f*). Since the external disturbance torque is applied during 4–4.2 s and 8–8.2 s, as shown in Fig. 6(*c*), the pendulum exhibits some deviations. However, the controller is robust enough to keep the states within the bounded neighborhood of the equilibrium point and bring them back to the desired values after the absence of the disturbance. Figures 6(*d*) and 6(*h*) show the estimations for the lumped "disturbance-like" terms. The good estimation guarantees the convergence of system tracking errors. Figure 6(*g*) depicts the input motor voltage.

6.3 Experimental Study: Level Control of a Coupled Water Tank System. A coupled water tank system as shown in Fig. 7 is composed of two coupled water tanks and two DC water pumps. The water levels in the two tanks are measured by the pressure sensors at the bottom and the two water pumps are powered by two single channel linear voltage amplifiers. The controller used in the experiment is the DSPACE DS1104 device with a 12-bit A/D converter. The system has a hardware resolution at 0.03 cm. The two pumps $P1$ and $P2$ are used to pump the two tanks 1 and 2, respectively. The pump 2 is considered as the control input and the water level of tank 1 is considered as the output. To add the mismatched disturbance into the system, the pump 1 is used to pump water into tank 1, consequently, the disturbance is not in the same channel with the control input.

The system dynamic model is expressed as

$$\dot{L}_1 = \frac{a_2}{A_1}\sqrt{2gL_2} - \frac{a_1}{A_1}\sqrt{2gL_1} + \frac{K_p}{A_1}\mathscr{D}(V_{p1}), \tag{67}$$

$$\dot{L}_2 = -\frac{a_2}{A_2}\sqrt{2gL_2} + \frac{K_P}{A_2}\mathscr{D}(V_{p2}), \tag{68}$$

Table 3 Parameters of the coupled water tank system

Parameters	a_1	a_2	g	A_1	A_2	K_p
Values	0.1781 cm^2	0.1781 cm^2	981 cm/s^2	15.5179 cm^2	15.5179 cm^2	3.3 $cm^3/s/V$

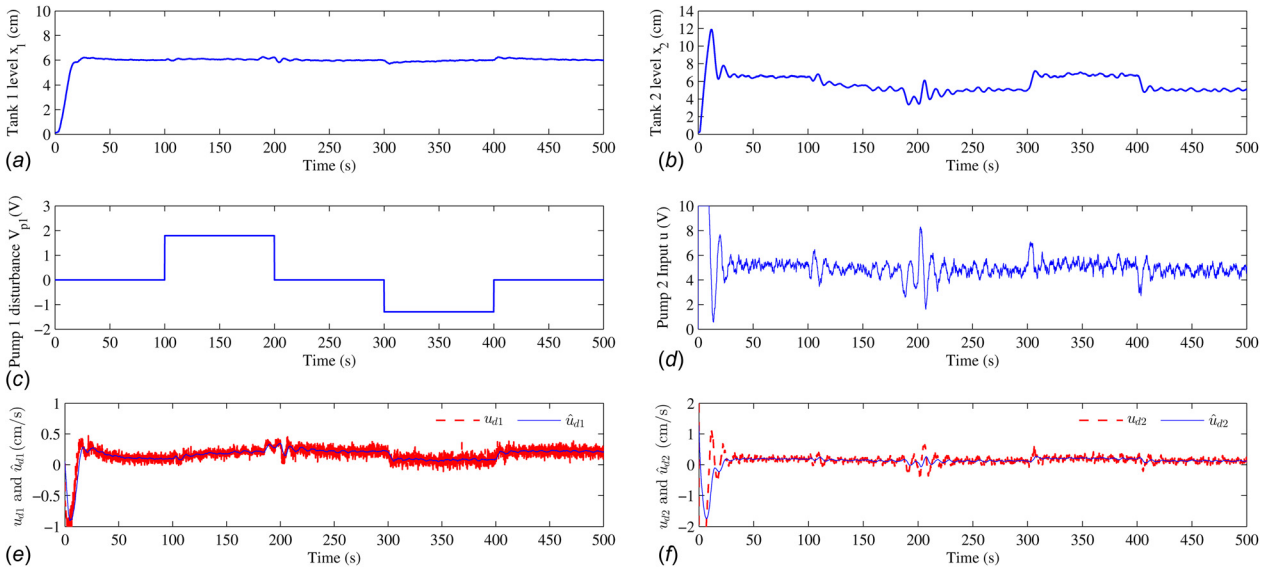

Fig. 9 Level control for a coupled water tank

where L_1 and L_2 are the water levels of tanks 1 and 2. V_{p1} and V_{p2} are the input voltages of two pumps. And $\mathscr{D}(\cdot)$ is a dead zone operator with unknown bounds. Other variables are summarized in the Table 3. Furthermore, the sensitivity of the water level sensor is 6.1 cm/V and the sampling time used in the experiment is set as 0.01 s. The maximal height of two tanks is at 25 cm, and the pump 2 can be operated in the range of [0 V, 10 V] and the pump 1 in the range of [−10 V, 10 V] .

The control objective is to maintain the water level of tank 1 at 6 cm, i.e., $L_1 = 6$ cm. One problem should be further mentioned is the dead-zone problem from which a water pump always suffers. As shown in Fig. 8, while the pump voltage V_{pi} is located inside the interval $[b_l, b_r]$, $\mathscr{D}(V_{pi})$ will be zero, $i = 1, 2$. For this experimental setup, b_l and b_r can be estimated to be around at −1 V and 1 V by experimental testing, respectively. In fact, the exact bound of the dead zone is usually unmeasurable. Therefore, let $\mathscr{D}(V_{p2}) = V_{p2} + d_{p2}$, where d_{p2} is regarded as a kind of system uncertainty

$$d_{p2} = \begin{cases} 0, & V_{p2} < b_l \\ -V_{p2}, & b_l \le V_{p2} \le b_r \\ 0, & V_{p2} > b_r \end{cases} \tag{69}$$

To formulate the control problem, let $x_1 = L_1$, $x_2 = L_2$, $u = V_{p2}$ and the reference signal x_{1r} is generated by $x_{1r} = \mathscr{L}^{-1}1/(10s+1) * 6$ cm. In addition, by using the Taylor's series, $\sqrt{2gx_2} = \sqrt{2gx_{1r}} + \sqrt{g/2x_{1r}}(x_2 - x_{1r}) + O(x_2^2)$, the systems (67) and (68) can be written in the following state space model in the form (17):

$$\dot{x}_1 = \bar{f}_1 + b_1 x_2 + \Delta f_1 + d_1 \tag{70}$$

$$\dot{x}_2 = \bar{f}_2 + b_u u + \Delta f_2 \tag{71}$$

where Δf_1 is the unknown higher-order term $O(x_2^2)$ and

$$\bar{f}_1 = -\frac{a_1}{A_1}\sqrt{2gx_1} + \frac{a_2}{A_1}\left(\sqrt{2gx_{1r}} - \sqrt{\frac{gx_{1r}}{2}}\right),$$
$$b_1 = \frac{a_2}{A_1}\sqrt{\frac{g}{2x_{1r}}},\ d_1 = \frac{K_p}{A_1}\mathscr{D}(V_{p1}),$$
$$\bar{f}_2 = -\frac{a_2}{A_2}\sqrt{2gx_2},\ b_u = \frac{K_p}{A_2},\ \Delta f_2 = \frac{K_p}{A_2}d_{p2}$$

The process starts when both tanks are empty, i.e., $x_1 = x_2 = 0$ cm, $\Delta f_1 + d_1$ is regarded as the mismatched uncertainty and disturbance and Δf_2 is the matched one. The lumped "disturbance-like" terms in the design process are $u_{d1} = b_1(z_2 + y_2) + \Delta f_1 + d_1$ and $u_{d2} = \Delta f_2$. According to the Algorithm 1, the UDE-based backstepping controller is designed by the following two steps:

Step 1. Let $z_1 = x_1 - x_{1r}$, the virtual control is

$$x_{2r} = \frac{A_1}{a_2}\sqrt{\frac{2x_{1r}}{g}}\left(-k_1 z_1 - \bar{f}_1 - \mathscr{L}^{-1}\left\{\frac{G_{f1}(s)}{1 - G_{f1}(s)}\right\} * (\dot{z}_1 + k_1 z_1)\right)$$

where $k_1 = 0.033$, $G_{f1}(s) = 1/(2s+1)$. Moreover, the reference model utilized here is $\dot{\omega}_{2r} = -\alpha_2\omega_{2r} + \beta_2 x_{2r}, \omega_{2r}(0) = x_{2r}(0) = 0$, where $\alpha_2 = \beta_2 = 1$.

Step 2. Let $z_2 = x_2 - \omega_{2r}$, the controller is

$$u = \frac{A_2}{K_p}\left[-k_2 z_2 - \bar{f}_2 - \alpha_2\omega_{2r} + \beta_2 x_{2r} - \mathscr{L}^{-1}\left\{\frac{G_{f2}(s)}{1 - G_{f2}(s)}\right\} * (\dot{z}_2 + k_2 z_2)\right]$$

where $k_2 = 0.08, G_{f2} = 1/(5s+1)$.

The error feedback gains should satisfy $k_2 > k_1$, which will guarantee the inner loop is faster than the outer loop in Fig. 1. As shown in Ref. [12], there exists a tradeoff about the choice of the bandwidths of $G_{fi}(s)$ between the good estimation of uncertainties and disturbances, and the mitigation of the measurement noise. The cut-off frequencies of $G_{fi}(s)$ are selected as low as 0.5 rad/s, 0.2 rad/s, due to the low frequency measurement noise in the system. The experimental results are shown in Fig. 9. As shown in Fig. 9(*c*), the external disturbance is generated by pump 1. During 100–200 s, $V_{p1} = 1.8$ V and during 300–400 s, $V_{p1} = -1.3$ V. The water levels for both tanks are shown in Figs. 9(*a*) and 9(*b*). Due to the robustness of the controller, the water level for tank 1, i.e., x_1, is seen to be stabilized at 6 cm in the presence of both mismatched and matched disturbances. As shown in Table 4, the maximum errors remain within 5% while the mismatched disturbance is applied; the RMS of the tracking errors for the different time intervals is close to 0.03 cm, which is the hardware resolution. The associated input voltage for pump 2, i.e., u, is shown in Fig. 9(*d*). The good estimations of the lumped "disturbance-like" terms are shown in Figs. 9(*e*) and 9(*f*). It is worth noticing that the

Table 4 System output performance

Time period	0–100 s	100–200 s	200–300 s	300–400 s	400–500 s
Percentage maximum error	3.65%	2.15%	3.82%	4.97%	4.15%
Time period	50–80 s	150–180 s	250–280 s	350–380 s	450–480 s
RMS of steady-state error (cm)	0.04	0.07	0.04	0.04	0.05

larger error during 300–400 s than during 100–200 s maybe caused by the nonsymmetric ($b_r \neq b_l$) dead zone nonlinearity of the pump. Intuitively, b_r and b_l are unknown but there maybe $|b_r| > |b_l|$, then $|1.8 - b_r| < |-1.3 - b_l|$ is possible. That means, the effect of the disturbance $V_{p1} = -1.3$ V during 300–400 s might be more significant than that of $V_{p1} = +1.8$ V during 100–200 s. The proposed control approach does not require the bound information of the disturbance. The external disturbance can be any type. As shown in the tuning guideline in Sec. 6.1, only the spectrum information of the disturbance is needed. The bound of the disturbance can be arbitrarily large as long as within the hardware limit, i.e., there is no saturation on the actuators. In practice, the bound of allowable disturbance is only restricted by the physical saturation of actuators.

7 Conclusion

To relax the structural constraint of the UDE-based control, the backstepping approach was adopted. The proposed strategy was applicable for a general type of nonlinear systems with mismatched uncertainties and disturbances. In the view of the UDE-based control, not only the uncertainties and disturbances but also the nonstrict-feedback terms, intermediate system errors were all lumped into the "disturbance-like" terms. Then, the lumped "disturbance-like" terms can be estimated and compensated. Besides the extension of the UDE-based control, two benefits for the backstepping approach were also presented. First, this method is applicable for a more general type of nonlinear systems which is not just in the strict-feedback form. Second, the utilization of reference models which inherits from the UDE-based method relaxes the "complexity explosion" problem. The tuning guideline was clarified based on a numerical example. At last, a simulation study based on a rotary inverted pendulum and an experimental study based on a coupled water tank system were carried out to show how to apply the proposed method to engineering applications.

Funding Data

- Directorate for Engineering (National Science Foundation, Grant No. CMMI 1728255).

References

[1] Youcef-Toumi, K., and Ito, O., 1990, "A Time Delay Controller for Systems With Unknown Dynamics," ASME J. Dyn. Syst. Meas. Control, **112**(1), pp. 133–142.

[2] Park, J. H., and Kim, Y. M., 1999, "Time-Delay Sliding Mode Control for a Servo," ASME J. Dyn. Syst., Meas., Control, **121**(1), pp. 143–148.

[3] Chang, P., Park, S.-H., and Lee, J.-H., 1999, "A Reduced Order Time-Delay Control for Highly Simplified Brushless Dc," ASME J. Dyn. Syst., Meas., Control, **121**(3), pp. 556–560.

[4] Chang, P. H., Park, B. S., and Park, K. C., 1996, "An Experimental Study on Improving Hybrid Position/Force Control of a Robot Using Time Delay Control," Mechatronics, **6**(8), pp. 915–931.

[5] Chang, P., and Lee, J., 1996, "A Model Reference Observer for Time-Delay Control and Its Application to Robot Trajectory Control," IEEE Trans. Control Syst. Technol, **4**(1), pp. 2–10.

[6] Youcef-Toumi, K., and Wu, S., 1992, "Input-Output Linearization Using Time Delay Control," ASME J. Dyn. Syst. Meas. Control, **114**(1), pp. 10–19.

[7] Zhong, Q.-C., and Rees, D., 2004, "Control of Uncertain LTI Systems Based on an Uncertainty and Disturbance Estimator," ASME J. Dyn. Syst. Meas. Control, **126**(4), pp. 905–910.

[8] Zhong, Q.-C., Kuperman, A., and Stobart, R., 2011, "Design of UDE-Based Controllers From Their Two-Degree-of-Freedom Nature," Int. J. Robust Nonlinear Control, **21**(17), pp. 1994–2008.

[9] Shendge, P., and Patre, B., 2007, "Robust Model Following Load Frequency Sliding Mode Controller Based on UDE and Error Improvement With Higher Order Filter," IAENG Int. J. Appl. Math., **37**(**1**), pp. 27–32.

[10] Chandar, T. S., and Talole, S. E., 2014, "Improving the Performance of UDE-Based Controller Using a New Filter Design," Nonlinear Dyn., **77**(3), pp. 753–768.

[11] Kuperman, A., 2015, "Design of α-Filter-Based Ude Controllers Considering Finite Control Bandwidth," Nonlinear Dyn., **81**(1–2), pp. 411–416.

[12] Ren, B., Zhong, Q.-C., and Dai, J., 2017, "Asymptotic Reference Tracking and Disturbance Rejection of UDE-Based Robust Control," IEEE Trans. Ind. Electron, **64**(4), pp. 3166–3176.

[13] Talole, S., and Phadke, S., 2010, "Robust Input-Output Linearisation Using Uncertainty and Disturbance Estimation," Int. J. Control, **82**(10), pp. 1794–1803.

[14] Talole, S., Chandar, T., and Kolhe, J. P., 2011, "Design and Experimental Validation of Ude Based Controller–Observer Structure for Robust Input–Output Linearisation," Int. J. Control, **84**(5), pp. 969–984.

[15] Talole, S., and Phadke, S., 2008, "Model Following Sliding Mode Control Based on Uncertainty and Disturbance Estimator," ASME J. Dyn. Syst. Meas. Control, **130**(3), pp. 1–5.

[16] Castillo, A., Sanz, R., Garcia, P., and Albertos, P., 2017, "Robust Design of the Uncertainty and Disturbance Estimator," IFAC-PapersOnLine, **50**(1), pp. 8262–8267.

[17] Deshpande, V., and Phadke, S., 2012, "Control of Uncertain Nonlinear Systems Using an Uncertainty and Disturbance Estimator," ASME J. Dyn. Syst. Meas. Control, **134**(2), p. 024501.

[18] Stobart, R. K., and Zhong, Q.-C., 2011, "Uncertainty and Disturbance Estimator-Based Control for Uncertain LTI-SISO Systems With State Delays," ASME J. Dyn. Syst. Meas. Control, **133**(2), pp. 1–6.

[19] Kuperman, A., and Zhong, Q.-C., 2010, "Robust Control of Uncertain Nonlinear Systems With State Delays Based on an Uncertainty and Disturbance Estimator," Int. J. Robust Nonlinear Control, **21**(1), pp. 79–92.

[20] Ren, B., Zhong, Q.-C., and Chen, J., 2015, "Robust Control for a Class of Non-Affine Nonlinear Systems Based on the Uncertainty and Disturbance Estimator," IEEE Trans. Ind. Electron, **62**(9), pp. 5881–5888.

[21] Sanz, R., Garcia, P., Zhong, Q.-C., and Albertos, P., 2016, "Robust Control of Quadrotors Based on an Uncertainty and Disturbance Estimator," ASME J. Dyn. Syst. Meas. Control, **138**(7), p. 071006.

[22] Chen, J., Ren, B., and Zhong, Q.-C., 2016, "UDE-Based Trajectory Tracking Control of Piezoelectric Stages," IEEE Trans. Ind. Electron, **63**(10), pp. 6450–6459.

[23] Kolhe, J. P., Shaheed, M., Chandar, T. S., and Taloe, S. E., 2013, "Robust Control of Robot Manipulators Based on Uncertainty and Diturbance Estimation," Int. J. Robust Nonlinear Control, **23**(1), pp. 104–122.

[24] Xiao, L., 2014, "Aeroengine Multivariable Nonlinear Tracking Control Based on Uncertainty and Disturbance Estimator," ASME J. Eng. Gas Turbines Power, **136**(12), p. 121601.

[25] Ren, B., Wang, Y., and Zhong, Q.-C., 2017, "UDE-Based Control of Variable-Speed Wind Turbine Systems," Int. J. Control, **90**(1), pp. 121–136.

[26] Kuperman, A., and Zhong, Q.-C., 2015, "UDE-Based Linear Robust Control for a Class of Nonlinear Systems With Application to Wing Rock Motion Stabilization," Nonlinear Dyn., **81**(1–2), pp. 789–799.

[27] Aharon, I., Shmilovitz, D., and Kuperman, A., 2015, "Robust Output Voltage Control of Multimode Non-Inverting DC–DC Converter," Int. J. Control, **90**(1), pp. 110–120.

[28] Wang, Y., Ren, B., and Zhong, Q.-C., 2016, "Robust Power Flow Control of Grid-Connected Inverters," IEEE Trans. Ind. Electron, **63**(11), pp. 6887–6897.

[29] Su, S., and Lin, Y., 2011, "Robust Output Tracking Control of a Class of Non-Minimum Phase Systems and Application to VTOL Aircraft," Int. J. Control, **84**(11), pp. 1858–1872.

[30] Sun, L., Li, D., Zhong, Q. C., and Lee, K. Y., 2016, "Control of a Class of Industrial Processes With Time Delay Based on a Modified Uncertainty and Disturbance Estimator," IEEE Trans. Ind. Electron, **63**(11), pp. 7018–7028.

[31] Krstić, M., Kanellakopoulos, I., and Kokotović, P. V., 1995, *Nonlinear and Adaptive Control Design*, Wiley, New York.

[32] Ikhouane, F., and Krstić, M., 1998, "Robustness of the Tuning Functions Adaptive Backstepping Design for Linear Systems," IEEE Tran. Autom. Control, **43**(3), pp. 431–437.

[33] Zhou, J., and Wen, C., 2008, *Adaptive Backstepping Control of Uncertain Systems: Nonsmooth Nonlinearities, Interactions or Time-Variations*, Springer, New York.

[34] Swaroop, D., Hedrick, J. K., Yip, P. P., and Gerdes, J. C., 2000, "Dynamic Surface Control for a Class of Nonlinear Systems," IEEE Trans. Autom. Control, **45**(10), pp. 1893–1899.

[35] Yip, P. P., and Hedrick, J. K., 1998, "Adaptive Dynamic Surface Control: A Simplified Algorithm for Adaptive Backstepping Control of Nonlinear Systems," Int. J. Control, **71**(5), pp. 959–979.

[36] Apkarian, J., Karam, P., and Levis, M., 2011, "Instructor Workbook: Inverted Pendulum Experiment for Matlab/Simulink Users," Quanser Inc, Markham, ON, Canada.